

Article

Nonoxidative Coupling of Methane to Produce C₂ Hydrocarbons on FLPs of an Albite Surface

Yannan Zhou^{1,2,*} , Ye Chen³, Xuegang Luo^{1,3,*} and Xin Wang³¹ Research Center of Laser Fusion, China Academy of Engineering Physics, Mianyang 621900, China² Qinghai Institute of Salt Lakes, Chinese Academy of Sciences, Xining 810008, China³ Engineering Research Center of Biomass Materials, Ministry of Education, Mianyang 621010, China

* Correspondence: yannanzhou87@163.com (Y.Z.); lxg@swust.edu.cn (X.L.)

Abstract: The characteristics of active sites on the surface of albite were theoretically analyzed by density functional theory, and the activation of the C-H bond of methane using an albite catalyst and the reaction mechanism of preparing C₂ hydrocarbons by nonoxidative coupling were studied. There are two frustrated Lewis pairs (FLPs) on the (001) and (010) surfaces of albite; they can dissociate H₂ under mild conditions and show high activity for the activation of methane C-H bonds. CH₄ molecules can undergo direct dissociative adsorption on the (010) surface, whereas a 50.07 kJ/mol activation barrier is needed on the (001) surface. The prepared albite catalyst has a double combination function of the (001) and (010) surfaces; these surfaces produce a spillover phenomenon in the process of CH₄ activation reactions, where CH₃ overflows from the (001) surface with CH₃ adsorbed on the (010) surface to achieve nonoxidative high efficiently C-C coupling with an activation energy of 18.51 kJ/mol. At the same time, this spillover phenomenon inhibits deep dehydrogenation, which is conducive to the selectivity of the C₂ hydrocarbons. The experimental results confirm that the selectivity of the C₂ hydrocarbons is maintained above 99% in the temperature range of 873 K to 1173 K.

Keywords: albite; frustrated Lewis pairs; methane; nonoxidative coupling on surface; doping modification of catalyst



Citation: Zhou, Y.; Chen, Y.; Luo, X.; Wang, X. Nonoxidative Coupling of Methane to Produce C₂ Hydrocarbons on FLPs of an Albite Surface. *Molecules* **2023**, *28*, 1037. <https://doi.org/10.3390/molecules28031037>

Academic Editors: Jorge Garza, Rubicelia Vargas and Andrei L. Tchougréeff

Received: 23 December 2022

Revised: 15 January 2023

Accepted: 16 January 2023

Published: 19 January 2023



Copyright: © 2023 by the authors. Licensee MDPI, Basel, Switzerland. This article is an open access article distributed under the terms and conditions of the Creative Commons Attribution (CC BY) license (<https://creativecommons.org/licenses/by/4.0/>).

1. Introduction

Direct conversion of methane (DMC) to high value-added chemicals (such as ethylene and other compounds) is an effective way to achieve its efficient utilization, which plays a vital role in the economy and environment. Methane is the most stable small molecule in nature, due to its stable tetrahedral symmetric structure, which causes its efficient activation and direct conversion under mild conditions to be extremely challenging. After decades of continuous efforts, researchers have proposed many ways to produce DMC, among which the development of oxidative coupling, nonoxidative dehydrogenation and selective oxidation methods has greatly promoted research on DMC. In recent years, the high utilization rate and high selectivity of the active species of single-atom catalysts (SACs) have attracted extensive attention from researchers [1–4]. Because of their unique catalytic performance in DMC reactions, SACs have been used in various reactions, and although they have many advantages, they still face many challenges, due to their high surface energy and instability of single atoms along with limitations of characterization methods for the nanoscale to single-atom scale species, catalyst design and preparation, etc. Therefore, the goal is to find catalysts with high catalytic performance, simple preparation and good stability.

Since 2006, Professor W. Stephan has found that homogeneous frustrated Lewis pair (FLP) catalysts could activate the H₂ molecule [5] under mild conditions, and the activation potential of FLP for small molecules in homogeneous fields has constantly been of great interest to researchers. However, the application of homogeneous FLPs is hindered by

defects such as product separation and the recycling of catalysts; some researchers have gradually begun focusing on developing heterogeneous FLP catalysts on a solid surface, aiming to make a breakthrough in DMC. At present, all-solid FLPs constructed from a variety of materials, such as doped graphene [6], B/Al-doped phosphorenes [7], and hydroxylated indium oxide [8], have shown good activity performance for H₂ activation and hydrogenation reactions. Since research in this area has just began, there have been relatively few studies on the nonoxidative activation of CH₄. Metal oxides such as the FLP of γ -Al₂O₃ (110) and CeO₂(110) have a remarkable ability to activate the methane C-H bond [9,10], and nonoxidative C-C coupling can be performed on the surface of CeO₂. Recently, researchers have extended the concept of FLP to multistage porous Ti-based and zeolite molecular sieve catalytic systems [11,12] and made important progress in the research of photocatalytic nonoxidative coupling of methane and dehydrogenation of hydrocarbons above C₃. To date, the reference research methods and concepts are very limited. However, solid FLPs show the potential to activate methane in catalytic reactions, which attract further research and exploration to achieve different goals in FLP research.

Albite (Ab) is a type of natural mineral that is abundant, cheap, and easy to obtain. It not only has good thermal stability and chemical stability but also has channel structure characteristics similar to those of zeolites. The difference is that the pore diameter of the channel is below 3 Å and belongs to the ultra-microchannel; due to this difference, researchers have not pursued long-term studies using albite. In an experimental study, we found that albite catalysts have a certain activation effect on methane using nonoxidative conditions, and the C₂ hydrocarbon selectivity is above 99% [13]. Using density functional theory (DFT), it is found that FLPs exist on the surface of albite, and we speculate that they activate methane according to the mechanism of FLPs. Therefore, it is necessary to further study the nature and trends of methane activation using albite catalysts in theory, which is of great significance to expand the application of ultra-microchannel mineral materials.

In this study, initially, the FLP active sites on the (001) and (010) surfaces of albite were theoretically analyzed, and the calculation confirmed that they had the characteristics of FLPs. Then, we studied in detail the activation effects and conversion behaviors of surface FLPs to CH₄ and determined the mechanism showing its high selectivity to C₂ hydrocarbons and its non-easy production in carbon deposits. Finally, the static electric field of FLPs was regulated by doping modification, and the influence on CH₄ conversion was analyzed and discussed to obtain a newfound understanding of the application of albite and provide a novel concept and method for the nonoxidative coupling of methane by solid FLPs.

2. Results and Discussion

2.1. Theoretical Analysis of FLP Sites on Albite Surfaces

The basic structural units of albite (NaAlSi₃O₈) are [SiO₄] and [AlO₄] tetrahedrons, and each oxygen atom in the skeleton is shared with two adjacent tetrahedrons. Because of the charge imbalance caused by Al replacing Si, a Na⁺ cation with balanced charge is introduced into the structure and is located in the pores of the tetrahedral skeletal structure. Albite minerals have two common exposed surfaces, (001) and (010), in a natural or grinding external force situation [14,15], and the structures are shown in Figure 1.

Initially, we analyzed the active sites in the two surface structures of albite according to Lewis acid–base theory. The tetrahedral central atoms in albite structures Al and Si have four sp³ hybrid orbitals, which are bonded to four O atoms on the (001) surface. [AlO₃] lacking one oxygen is exposed on the surface layer. Al is in the coordination unsaturated state and has an empty orbital, which can accept electron pairs; Al acts as a Lewis acid (LA). The oxygen atom exposed on the surface has an electron rich attribute and acts as a Lewis base (LB). [SiO₃] lacking oxygen is exposed on the (010) surface. Si is in the coordination unsaturated state, its valence orbit can accept electrons, and it acts as a LA; similarly, the oxygen atom exposed to the surface acts as a LB. Both LAs and LBs on the two surfaces are distributed on the skeleton of [AlO₄] and [SiO₄]. The formation of solid frustrated Lewis

acid–base pairs requires not only independent LAs and LBs but also appropriate sterically encumbered matching pairs. Albite is a mineral with an ultra-microchannel structure, and the pore diameter parallel to the channel is mainly below 0.3 nm [16–18]. Due to its undulating and uneven surface, many micropores are formed that are not parallel to the crystal surface; that is, the Lewis acid and base sites distributed on the surface skeleton of albite are not in the same horizontal plane. On the (001) surface, there were two sterically encumbered combinations: one group was located on the channel skeleton, with a distance of 4.21 Å, and the other group was located on the pore skeleton, with a distance of 4.39 Å. On the (010) surface, there were also two combinations: the distance on the channel skeleton was 5.10 Å, and the distance on the pore skeleton was 4.20 Å. Using the viewpoint that a distance between Lewis acid–base sites of approximately 4 Å is appropriate [12,19,20], the Lewis acid–base pairs on the channel skeleton of the (001) face and the pore skeleton of the (010) face are matched; therefore, there are FLPs on both surfaces of albite.

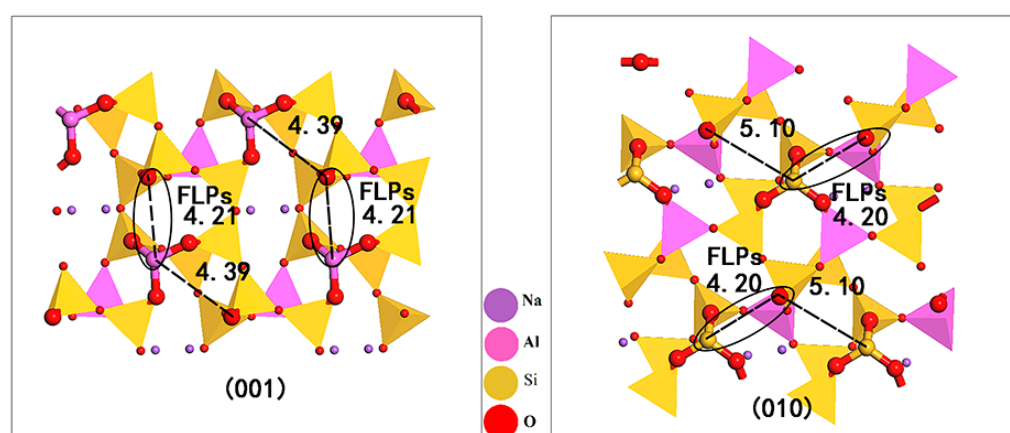


Figure 1. Schematic diagram of the albite (001) and (010) surface model. The circle indicates the FLPs position and the dotted lines indicates the distance between Lewis acid and Lewis base.

Second, to further verify the characteristics of FLPs on the surface of albite, we calculated the reaction barrier for activating H_2 (see Figure 2). The results showed that FLPs on both surfaces could enable H_2 heterolysis. The dissociation activation energy of the (001) surface was 36.48 kJ/mol, and that of the (010) surface was 1.01 kJ/mol. Heterolysis fragments of H^- and H^+ were adsorbed on the LA and LB, respectively. Erker et al. studied the activation mechanism of small molecules H_2 by FLPs and thought that the activation of small molecules by FLPs was based on the polarization of the electrostatic field between the electron receptor and donor acid–base pair [21,22]. Using a Lewis acid–base electrostatic field, an activity region would be formed, and the energy barrier in the reaction process was generated in the preparatory entry stage of small molecules. Once small molecules entered the active region of FLPs, the reaction energy barrier disappeared, and a stable dissociated product was finally formed [23]. We also found in the calculation that when H_2 is at a suitable distance from the Lewis acid–base pair on the two surfaces, direct dissociation adsorption occurs. When H_2 enters the active region formed by LA and LB, it is directly dissociated. The transition-state (TS) structure of H_2 dissociation (Figure 2) shows that the H_2 molecule has not been dissociated; in fact, the activation energies of 36.48 kJ/mol and 1.01 kJ/mol are required for H_2 to enter the activity region from outside. The FLPs on the two surfaces have a strong activation effect on H_2 , showing evident FLP characteristics. Thus, albite is a natural mineral with an ultra-microchannel structure, and its surface coordination unsaturated Si, Al, and O atoms are distributed on the skeleton formed by $[AlO_4]$ and $[SiO_4]$, which can form mutually independent LAs and LBs. Its ultra-microchannel structure causes the LAs and LBs to form matching subnanoscale sterically encumbered minerals, thus forming FLPs.

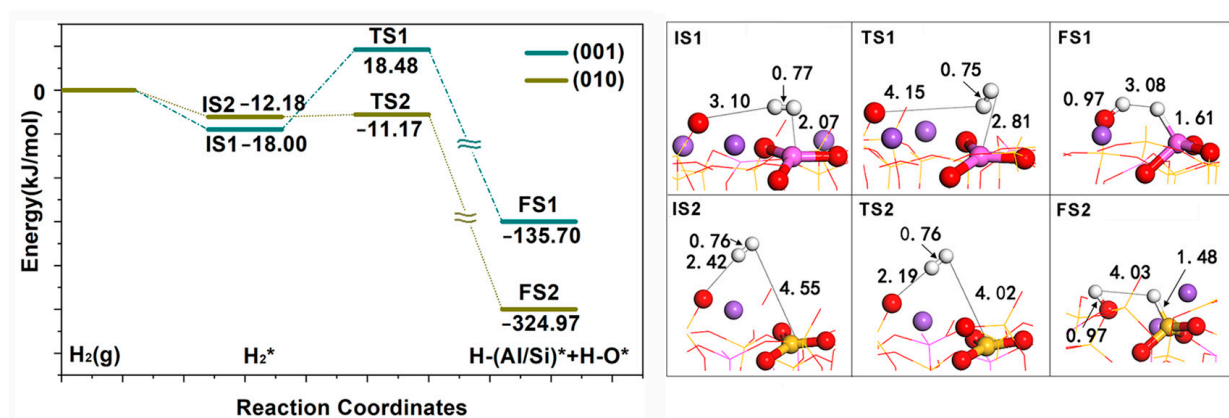


Figure 2. Geometric structures of the transition state intermediates of dissociation reactions of H_2 on the FLP of $NaAlSi_3O_8$ (001) and (010) surfaces. * indicates adsorption state, (g) indicates in gas phase state.

2.2. Effect on C-H Bond Activation of Methane

To deeply understand the adsorption and activation mechanism of CH_4 on the FLPs of the albite surface, we initially calculated the adsorption energies of CH_4 , CH_3 , H and CH_3/H on the two surfaces (see Table 1). Using the table, the most stable CH_4 is adsorbed on the LA (Al,Si), and the most stable adsorption of the co-adsorption system of CH_4 dissociated species CH_3/H is located on the LA (Al,Si)/LB (O). Additionally, the adsorption energies of CH_4 and dissociated species CH_3 , H on the two surfaces follow the trend of $CH_4 < CH_3 < H$. The adsorption of CH_3 and H on the (010) surface is stronger than that on the (001) surface, and their adsorption energies are 150.09 kJ/mol and 102.4 kJ/mol higher, respectively. The adsorption of CH_4 on the two surfaces had a similar phenomenon to that of H_2 , showing different adsorption between the CH_4 and LA (Al,Si) distances and degrees of polarization, as shown in Figure 3. On the (001) surface, when CH_4 is far from the LA (Al) site ($d_{C-Al} > 3.8 \text{ \AA}$), the adsorption energy is positive, indicating instability (see Figure 3a). When CH_4 is close to the LA (Al) site ($d_{C-Al} < 3.8 \text{ \AA}$), CH_4 is stably adsorbed at a position of 2.34 \AA from C to Al (see Figure 3b). The adsorption energy is -27.86 kJ/mol , generating a dipole moment of 0.13 D, indicating that CH_4 has been polarized; the C-H bond is weakened and stretched to 1.11 \AA . On the (010) surface, when CH_4 is far from the LA (Si) site ($d_{C-Si} > 3.9 \text{ \AA}$), the adsorption of CH_4 on the surface is weak (see Figure 3c). When CH_4 is close to the LA (Si) site ($d_{C-Si} < 3.9 \text{ \AA}$), heterolysis occurs directly, CH_3 is adsorbed on the LA (Si), and H is adsorbed on the LB (O), as shown in Figure 3d. This is completely consistent with the phenomenon described by Grimme S. et al., in that “once the molecule enters the hole of FLPs, the reaction proceeds without a barrier” [23]; that is, CH_4 can undergo direct dissociative adsorption in the active area of the Lewis acid–base pairs on the (010) surface.

Table 1. CH_4 , CH_3 , H, and CH_3/H adsorption energy of the Ab surface (kJ/mol).

Adsorbate	(001)		(010)	
	Sites	Adsorption Energy	Sites	Adsorption Energy
CH_4	LA	-27.86	LA	-12.4
	LB	-9.31	LB	-5.85
CH_3	LA	-252.83	LA	-402.92
	LB	-273	LB	-373.29
H	LA	-281.9	LA	-416
	LB	-394.44	LB	-496.84
CH_3/H	LA/LB	-723.37	LA/LB	-924.25
	LB/LA	-647.39	LB/LA	-817.08

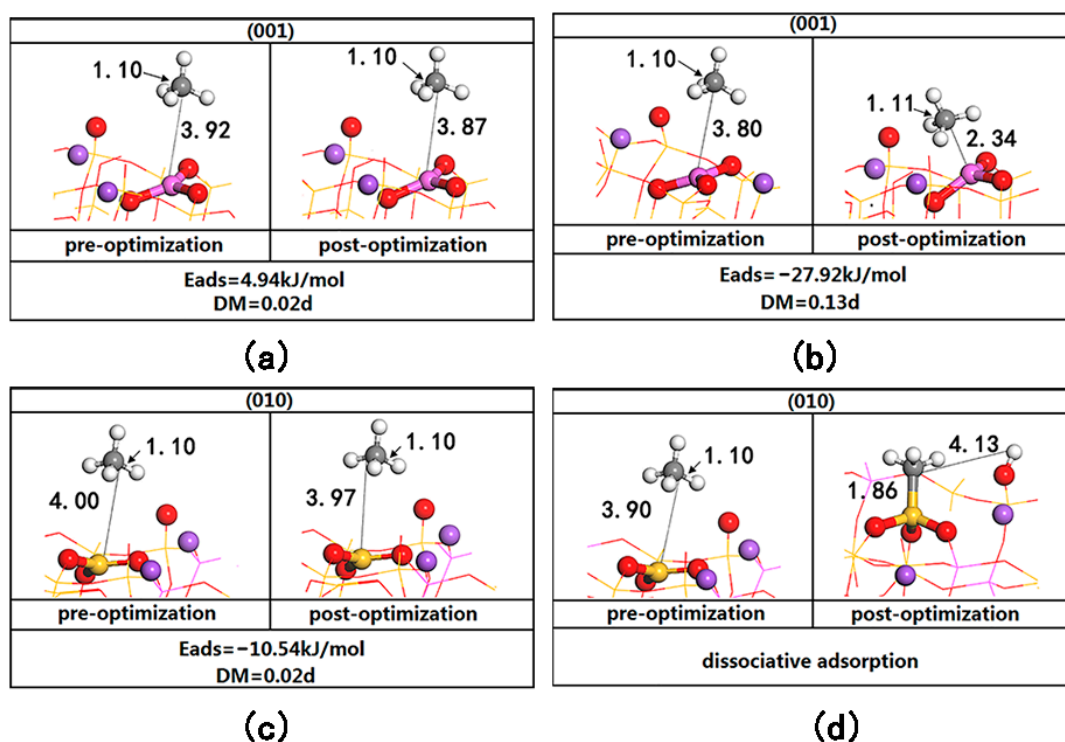


Figure 3. Adsorption configuration of CH₄ before and after (001) and (010) surface optimization. (a) is the adsorption configuration before and after optimization when (001) surface $d_{C-Al} = 3.92$ Å. (b) is the adsorption configuration before and after optimization when (001) surface $d_{C-Al} = 3.80$ Å. (c) is the adsorption configuration before and after optimization when (010) surface $d_{C-Si} = 4.00$ Å. (d) is the adsorption configuration before and after optimization when (010) surface $d_{C-Si} = 3.90$ Å.

To analyze the micro-mechanism of its dissociative adsorption process, we observed the dynamic change in the (010) surface adsorption configuration, as shown in Figure 4, and the corresponding Hirshfeld charge distribution and CH₄ dipole moments were calculated (see Table 2). Interestingly, there are three stages in the dissociative adsorption process of CH₄. In the first stage (a–d), as CH₄ gradually approaches the LA (Si), the LA (Si) is in a state of acquiring electrons, CH₄ is in a state of donating electrons, and the LB (O) has no electron transfer; the CH₄ dipole moment gradually increases, and CH₄ is in a state of physical adsorption. In the second stage (e–f), when the distance between C and Si is 2.23 Å, CH₄ chemisorbs with the LA (Si). At this time, the LA (Si) still maintains a state of acquiring electrons, the LB (O) begins to enter a state of donating electrons, and the dipole moment of CH₄ rapidly increases from 0.24 D to 0.57 D. The C–H bond closest to the LB (O) is stretched to 1.23 Å. In the third stage (g–h), when the C–H bond is stretched to 1.34 Å, the C–H bond is broken, and the H–LB (O) bond forms at the same time. After reaching a stable state, CH₃ and H are adsorbed on the LA (Si) and the LB (O), respectively, with charges of -0.07 e and $+0.18$ e. Based on the above reaction details, when CH₄ is adsorbed on the LA (Si) on the albite (010) surface, LA (Si) can obtain electrons and has strong electrophilicity. Therefore, it initially attacks the electron-enriched C atom in CH₄, causing the electrons from the CH₄ bonding orbital σ to flow to the LA (Si) on the surface to form a Si–CH₄ intermediate; the C–H bond of CH₄ is weakened, which then promotes the nucleophilic attack of the LB (O) and provides electrons to the antibonding orbital σ^* of the C–H bond of CH₄ until it ruptures. In the process of CH₄ activation, the LA, as an electrophilic reagent, plays an important role in the polarization of CH₄; a greater degree of polarization of CH₄ correlates to a stronger reaction activity. The LB, as a nucleophilic reagent, can obtain protons, and they synergistically complete the cleavage of CH₄. Since the electrophilicity of the LA on the (001) surface is weaker than that on the (010) surface, its polarization to CH₄ is relatively weak, and CH₄ cannot be directly cleaved.

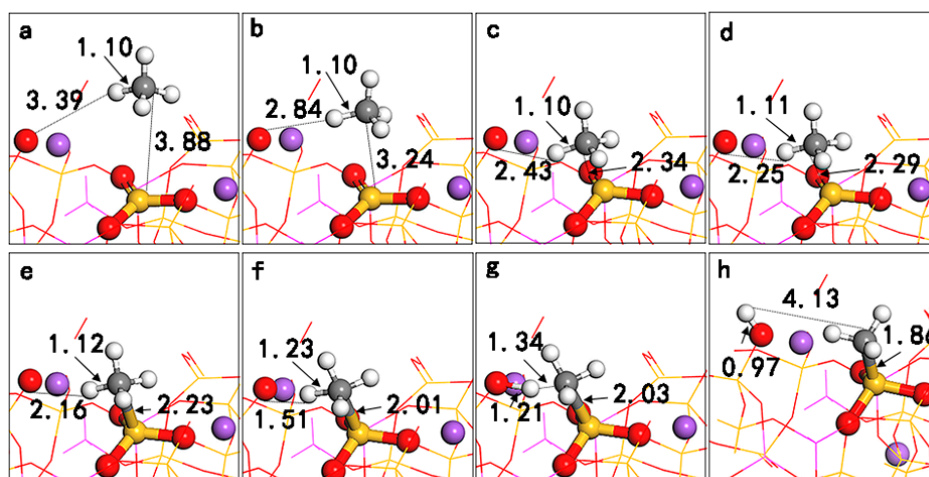


Figure 4. Surface dissociative adsorption process diagram of CH₄ on NaAlSi₃O₈ (010) (a–h).

Table 2. Hirshfeld charge distribution and dipole moments of the CH₄ dissociative adsorption process on the NaAlSi₃O₈ (010) surface.

State	Hirshfeld Charge Distribution (e)					CH ₄ di-Moments (Deby)
	LA(Si)	LB(O)	CH ₄	CH ₃	H	
a	0.71	−0.45	0.01	-	-	0.01
b	0.70	−0.45	0.03	-	-	0.04
c	0.61	−0.46	0.22	-	-	0.16
d	0.61	−0.45	0.23	-	-	0.19
e	0.60	−0.45	0.24	-	-	0.24
f	0.56	−0.40	0.21	-	-	0.57
g	0.55	−0.33	-	0.05	0.08	-
h	0.50	−0.26	-	−0.07	0.18	-

Second, the reaction barriers of CH₄ activation by two surface FLPs were calculated (see Figure 5); both surfaces show good activity. The reaction heat of CH₄ dissociation on the (001) surface is −71.72 kJ/mol, and an activation energy of 50.07 kJ/mol needs to be overcome. The reaction heat of CH₄ dissociation on the (010) surface is −292.61 kJ/mol, and the activation energy is 2.63 kJ/mol. From the two surface TS structures, CH₄ on the (001) surface has been dissociated, while CH₄ on the (010) surface has not been dissociated. CH₄ was polarized and contained the activation energy required for methane to enter the activity region from outside. Once CH₄ enters the activity region, heterolysis occurs according to the direct dissociation mechanism.

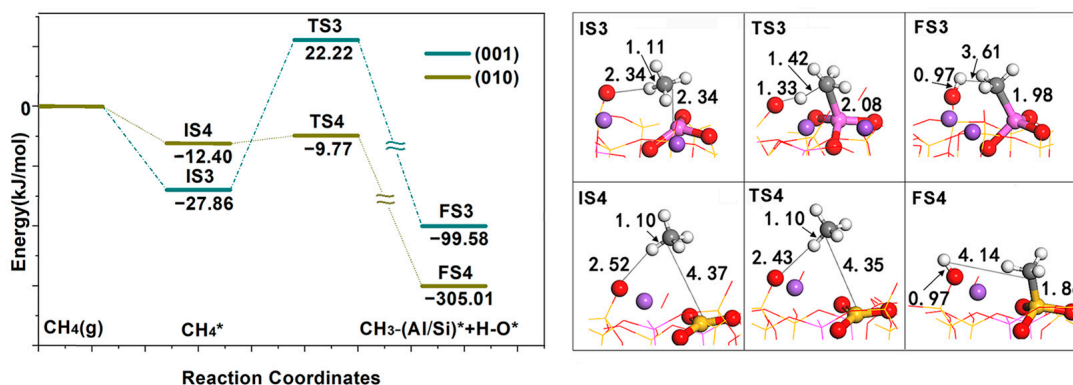


Figure 5. Geometric structures of the transition state intermediates of the activation reactions of CH₄ on the FLP of NaAlSi₃O₈ (010) and (001) surfaces. * indicates adsorption state, (g) indicates in gas phase state.

From a thermodynamic point of view, the dissociation reaction heat of the (010) surface is far greater than that of the (001) surface, indicating that the bonding effect between dissociated fragments CH_3 and H with acid–base sites of the (010) surface is stronger than that of the (001) surface. From a kinetic point of view, the activation energy of CH_4 on the (010) surface is much lower than that on the (001) surface. Although the dissociation activation energy of CH_4 on the (010) surface is the lowest, the strong bonding effect between CH_3/H and the surface means that desorption requires a higher desorption energy, which is in accordance with the Brønsted Evans Polanyi rule [24].

2.3. Effect on the Methyl C-C Coupling Mode

The albite catalyst is prepared by high-temperature calcination and grinding using an external force to physically mix and fully expose the two common exposed surfaces, (001) and (010). In fact, it is a double combination catalyst with (001) and (010) coexisting, and they participate in the catalytic reaction of methane at the same time. Figure 6 shows the catalytic conversion path of methane on the albite catalyst; when methane enters the catalyst surface from the gas phase, the FLPs on both surfaces cause methane heterolysis according to the same activation mechanism, and the dissociated fragments CH_3 and H are located on LA and LB sites on both surfaces, respectively. Since the bonding effect with CH_3 and H adsorbed on the (001) surface is much weaker than that on the (010) surface, they preferentially desorb during temperature rise desorption, causing a spillover phenomenon; at the same time, because the Lewis acid site Al on the (001) surface has an empty orbital and CH_3^- has a lone electron pair, after the two bond, that is, CH_3^- adsorbed on (001) surface can neither give nor gain electrons, C-C coupling does not occur on (001) surface. Similarly, the spilled H^+ cannot gain electrons from Lewis acid site Al in (001) surface to form H^- . Therefore, the coupling reaction of CH_3 and H overflows on (001) surface can only occur on (010) surface, that is, CH_3 and H preferentially desorbed become overflows and diffuse to the (010) surface with an increase in the concentration gradient. In the overflow process, since the bonding effect of CH_3 on the (001) surface is much smaller than that of H , CH_3 desorbs first.

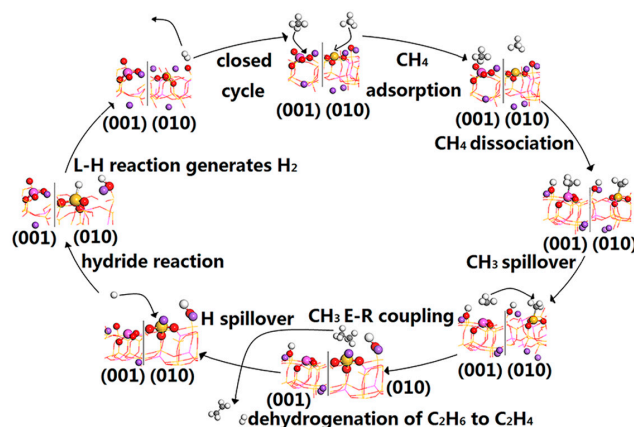


Figure 6. Schematic diagram of the path for activation and conversion of CH_4 by albite catalyst.

Figure 7 shows the desorption energy of CH_3 spillover and H spillover on the (001) surface and the reaction energy barrier on the (010) surface. The desorption of CH_3 requires an activation energy of 306.37 kJ/mol, and the diffusion to the (010) surface is coupled with the adsorbed methyl group through the E-R mechanism. The formation of C_2H_6 is an exothermic process and only requires an activation energy of 18.51 kJ/mol, indicating that C-C coupling has a strong bonding effect and shows good activity. CH_3 is E-R coupled on the surface, which is advantageous both in thermodynamics and kinetics, and part of the C_2H_6 generated by coupling continues to dehydrogenate and then generates C_2H_4 . The above results are consistent with the experimental results. At 1073 K, the analysis of the relationship between CH_4 conversion, C_2 hydrocarbon selectivity and space velocity

(GHSV) shows that CH_4 conversion decreases with increasing GHSV; CH_4 activation is fully achieved on the surface FLPs because a higher GHSV corresponds to a shorter contact time and lower CH_4 conversion rate. The phenomenon of increasing C_2H_6 and decreasing C_2H_4 with increasing GHSV further confirms that the coupling of CH_3 to produce C_2H_6 occurs on the surface rather than in the gas phase. C_2H_4 is the product of dehydrogenation of C_2H_6 in the gas phase [13]. When H overflows and diffuses to the (010) surface, and since the electronegativity of the H atom (2.1) is greater than that of the Si atom (1.8), H spillover can easily acquire unpaired electrons from the LA (Si) to form H^- . This reaction process produces a strong exothermic reaction with a reaction heat of -431.12 kJ/mol and an activation energy of 24.69 kJ/mol. After that, H adsorbed on the LA (Si) reacts with proton H adsorbed on the LB (O) to generate H_2 through the L-H mechanism; the required activation energy is 306.08 kJ/mol, and the closed cycle of methane conversion is completed. Since the desorption energy required for H spillover on the (001) surface (387.36 kJ/mol) is the highest during the whole reaction process, this is the rate-determining step in the whole cycle process.

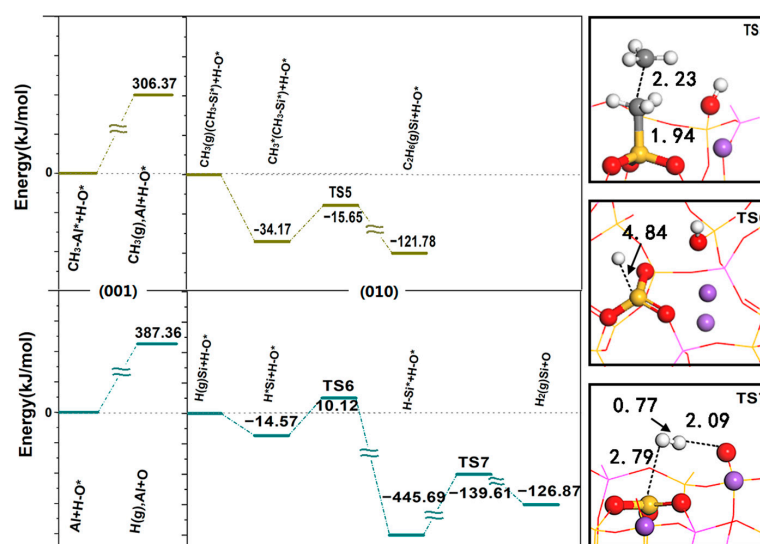


Figure 7. Diagram of desorption energy of CH_3 spillover and H spillover on the (001) surface and potential energy of reaction on the (010) surface. Corresponding structures of the transition state intermediates in the reaction path calculation. * indicates adsorption state, (g) indicates in gas phase state.

This spillover phenomenon not only enables highly efficient coupling of methyl groups but also plays two important roles: (1) to remove CH_3 and H, which are firmly adsorbed on the surface of (010), to regenerate the acid–base sites and (2) to avoid deep dehydrogenation, which is conducive to the selectivity of C_2 hydrocarbons. Because the heterolytic activation of CH_4 by FLPs on the surface of albite is a synergistic catalytic mechanism, the dehydrogenation activation of methane can only be achieved using the joint action of the LAs and LBs. After the Lewis acid–base sites are regenerated, the methane conversion cycle reaction can continue; the desorption order of the dissociated fragments adsorbed on the Lewis acid–base sites directly affects the reaction direction of conversion. When the LB site preferentially regenerates, the carbon species adsorbed on the LA site undergo dehydrogenation, whereas when the carbon species adsorbed on the LA site preferentially desorb, the occurrence of deep dehydrogenation is avoided. Since the bonding effect between the (001) face of CH_3 and the surface is much smaller than that of H, the preferential desorption of CH_3 avoids further dehydrogenation. At the same time, CH_3 preferentially overflowed is coupled on the (010) surface to form ethane, which also avoids further dehydrogenation of CH_3 adsorbed on the (010) surface. This reasonably explains

the experimental results that the selectivity of C₂ hydrocarbons is maintained across up to 99% and there are zero carbon deposits in the temperature range of 873~1173 K.

2.4. Effect of Doping Modification on CH₄ Conversion

From the above analysis, the albite catalyst shows good catalytic ability for methane C-H bond activation and methyl C-C coupling, has high selectivity for C₂ hydrocarbons and does not easily undergo carbon deposition. However, we also find that the conversion of CH₄ is relatively low, and it increases with increasing temperature. This phenomenon shows that the conversion of CH₄ is closely related to temperature. Since the FLP catalytic reaction is generally a synergistic mechanism, the regeneration of acid–base sites is crucial to the cyclic reaction. For albite catalysts, the desorption of dissociated fragment H on the (001) surface is the rate-determining step of the cyclic catalytic reaction. Under nonoxygen conditions, temperature is the main factor affecting the desorption of H, and higher desorption energy can lead to lower conversion. Therefore, on the basis of a lower desorption energy of CH₃ than that of H, a reduction in the desorption energy of H helps to improve methane conversion. In the albite structure, the Na⁺ in the pores mainly balances the residual negative charges on the skeleton and affects the electrostatic field formed by the LA and LB. According to the principle of field strength superposition, doping high valence metal ions instead of Na⁺ plays a role in regulating the electrostatic field of FLPs. In this experiment, we mixed the prepared albite catalyst with anhydrous lead chloride in different proportions, calcined it at 773 K, and formed a Pb²⁺-doped Pb/Ab catalyst through ion exchange. To investigate the influence of Pb doping on the CH₄ conversion rate, we calculated the desorption energy of H and CH₃ before and after (001) surface doping, and the calculated results were analyzed and compared with the experimental values of CH₄ conversion and C₂ hydrocarbon selectivity before and after doping at 1073 K (see Figure 8). The desorption energy of CH₃ after doping is still less than that of H, and the activation barrier of CH₄ is slightly increased, increasing from 50.07 kJ/mol to 59.21 kJ/mol; this result means that doping has less effect on the catalytic activity of CH₄, and the desorption energy of H is reduced from 387.36 kJ/mol to 337.46 kJ/mol, showing a decrease of 49.9 kJ/mol. Corresponding to the experimental results at 1073 K, the conversion of methane after doping was promoted by 2.45 times from 3.32% to 8.12%, and the selectivity remained above 99%. After doping, reducing the bonding effect of the (001) surface H has an evident effect on improving the conversion of CH₄. Therefore, we believe that a nonreduction (or very low reduction) in the activity and a smaller desorption energy of the CH₃ spillover than that of the H spillover using modification maximumly reduces the bonding effect between H and the surface to greatly improve the conversion rate. The above are our preliminary research results, and the application of albite catalysts requires further in-depth research.

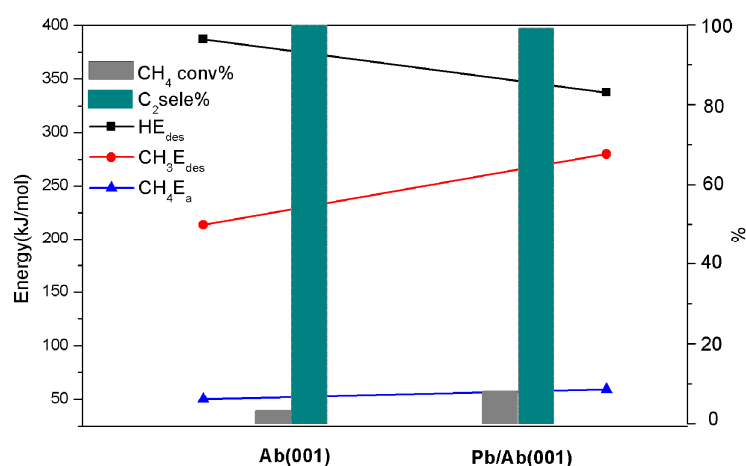


Figure 8. Effect of desorption energy of CH₃ and H, activation energy of CH₄ dissociation on CH₄ conversion and C₂ selectivity (1073 K) before and after doping on the (001) surface.

3. Calculation Method

In this paper, the DMol³ module [25] of MS19.1 software was used for simulation, and DFT was used for calculation. The exchange correlation potential is described by the PBE (Perdew, Burke and Enzerhof) function under the generalized gradient approximation GGA [26]. The electron wave function used the dual atomic orbital plus the polarization function DNP [25] as the basis set, and the truncation radius was 5.2 Å. The convergence tolerance of energy, gradient and displacement were 1.0×10^{-5} Ha, 0.002 Ha/Å and 0.005 Å, respectively. In the self-consistent functional (SCF) calculation, the convergence criterion was 1.0×10^{-6} Ha, and the smearing value was set to 0.005 Ha. The transition state was determined by the complete LST/QST [27] and nudged elastic band method (NEB) [28]. The atomic charge was calculated by Hirshfeld population analysis.

Albite crystals belong to the triclinic system, space group C_1 , and the lattice constants are $a = 0.8137$ nm, $b = 1.2787$ nm, $c = 0.7157$ nm, $\alpha = 94.245^\circ$, $\beta = 116.605^\circ$, and $\gamma = 87.809^\circ$ [29]. In this paper, surface models of periodic NaAlSi₃O₈ (001) and (010) were constructed as research objects. Both the (001) surface and (010) surface supercell models were $2 \times 1 \times 1$; this size ensured that there was no interaction between adsorbed molecules. A vacuum layer of 18 Å ensured that there was no interaction between adjacent albite layers in the z-axis direction. The k point parameters of the (001) surface and (010) surface were $2 \times 2 \times 1$ and $3 \times 3 \times 2$, respectively. The upper part and the adsorbate relaxed, while the remaining atoms were fixed in their original crystal positions. The doping calculation used Pb atoms to replace Na atoms in NaAlSi₃O₈ pores, and the DFT semicore pseudopotentials (DSPP) core treatment [30] was applied.

4. Conclusions

The effect of albite catalyst FLPs on the nonoxidative coupling of CH₄ was experimentally studied by DFT. The results show that the LA and LB formed on the (001) and (010) surfaces are sterically encumbered by approximately 4 Å due to albite having a unique ultra-microchannel structure and showing significant FLP characteristics. The activity region formed by the electrostatic field of Lewis acid–base pairs could enable H₂ heterolysis. Additionally, it has remarkable activation ability for methane C-H bonds, causes direct dissociative adsorption of CH₄ molecules in the active region of the (010) surface, and requires only a 50.07 kJ/mol energy barrier for the dissociation on the (001) surface. The albite catalyst prepared by sintering and grinding is a catalyst with coexisting (001) and (010) surfaces. The bonding effect of the dissociated species CH₃ with the two surfaces exhibits quite a larger difference; therefore, a spillover effect is triggered during temperature rise desorption. This spillover effect enables CH₃ to achieve highly efficient C-C coupling under nonoxidative conditions according to the E-R mechanism and can avoid deep dehydrogenation, inhibit carbon deposits, and maintain high selectivity of the C₂ hydrocarbons. The desorption of H spillover on the (001) surface is a key step in the CH₄ conversion cycle reaction, and its high desorption energy is the main reason that affects the conversion rate. By doping high valence metal ions, the nucleophilic and electrophilic properties of FLPs can be adjusted, the desorption energy of H can be reduced, the cycle reaction of methane conversion can be accelerated, and the conversion rate can be effectively doubly promoted. Albite, as a natural mineral with an ultra-microchannel structure, is not only abundant, inexpensive, and easy to obtain but also has good chemical and thermal stability. Moreover, the catalyst is simple to prepare, easy to recover and reuse, showing excellent properties for activation of the C-H bond of methane and C-C coupling, as well as high selectivity for C₂ hydrocarbons. This study not only provides a newfound understanding of mineral materials with ultra-microchannel structures but also provides a novel concept and reference for the further use of ultra-microchannel materials to construct new solid FLP catalysts and for the nonoxidative conversion of methane.

Author Contributions: Conceptualization, X.L.; methodology, X.L.; formal analysis, X.L.; investigation, Y.C. and X.W.; data curation, Y.C. and X.W.; writing—original draft preparation, X.L. and Y.Z.; writing—review and editing, Y.Z.; visualization, Y.Z. All authors have read and agreed to the published version of the manuscript.

Funding: This research was funded by National Transformation Program for Agricultural Science and Technology, and the grant number was (No. 2012GB2G200469).

Institutional Review Board Statement: Not applicable.

Informed Consent Statement: Not applicable.

Data Availability Statement: Not applicable.

Acknowledgments: This research was partially supported by China Academy of Engineering Physics of Research Center of Laser Fusion, Ministry of Education of Engineering Research Center of Biomass Materials, Institute of Salt Lakes of Chinese Academy of Science of Salt Lake Geology and Environment Laboratory.

Conflicts of Interest: The authors declare no conflict of interest.

References

1. Li, Y.; Hao, J.; Song, H.; Zhang, F.; Bai, X.; Meng, X.; Zhang, H.; Wang, S.; Hu, Y.; Ye, J. Selective light absorber-assisted single nickel atom catalysts for ambient sunlight-driven CO₂ methanation. *Nat. Commun.* **2019**, *10*, 2359. [CrossRef] [PubMed]
2. Bai, S.; Liu, F.; Huang, B.; Li, F.; Lin, H.; Wu, T.; Sun, M.; Wu, J.; Shao, Q.; Xu, Y.; et al. High-efficiency direct methane conversion to oxygenates on a cerium dioxide nanowires supported rhodium single-atom catalyst. *Nat. Commun.* **2020**, *11*, 954. [CrossRef] [PubMed]
3. Li, Z.; Xiao, Y.; Chowdhury, P.R.; Wu, Z.; Ma, T.; Chen, J.; Wan, G.; Kim, T.H.; Jing, D.; He, P.; et al. Direct methane activation by atomically thin platinum nanolayers on two-dimensional metal carbides. *Nat. Catal.* **2021**, *4*, 882–891. [CrossRef]
4. Wang, D.; Ding, X.; Liao, H.; Dai, J. Methane activation on (Au/Ag)₁-doped vanadium oxide clusters. *Acta Phys. Chim. Sin.* **2019**, *35*, 1005–1013. [CrossRef]
5. Welch, G.C.; Juan, R.R.S.; Masuda, J.D.; Stephan, D.W. Reversible, metal-free hydrogen activation. *Science* **2006**, *314*, 1124–1126. [CrossRef]
6. Sun, X.; Li, B.; Liu, T.; Song, J.; Su, D.S. Designing graphene as a new frustrated lewis pair catalyst for hydrogen activation by Co-doping. *Phys. Chem. Chem. Phys.* **2016**, *18*, 11120–11124. [CrossRef]
7. Zhao, J.; Liu, X.; Chen, Z. Frustrated lewis pair catalysts in two dimensions: B/Al-doped phosphorenes as promising catalysts for hydrogenation of small unsaturated molecules. *ACS Catal.* **2016**, *7*, 766–771. [CrossRef]
8. Wang, L.; Yan, T.; Song, R.; Sun, W.; Dong, Y.; Guo, J.; Zhang, Z.; Wang, X.; Ozin, G.A. Room temperature activation of H₂ by a surface frustrated lewis pair. *Angew. Chem. Int. Ed. Engl.* **2019**, *58*, 9501–9505. [CrossRef]
9. Wischert, R.; Copéret, C.; Delbecq, F.; Sautet, P. Optimal water coverage on alumina: A key to generate lewis acid–base pairs that are reactive towards the C–H bond activation of methane. *Angew. Chem. Int. Ed.* **2011**, *50*, 3202–3205. [CrossRef]
10. Huang, Z.; Zhang, T.; Chang, C.; Li, J. Dynamic frustrated lewis pairs on ceria for direct nonoxidative coupling of methane. *ACS Catal.* **2019**, *9*, 5523–5536. [CrossRef]
11. Ma, J.; Zhang, Q.; Chen, Z.; Kang, K.; Pan, L.; Wu, S.; Chen, C.; Wu, Z.; Zhang, J.; Wang, L. Design of frustrated lewis pair in defective TiO₂ for photocatalytic non-oxidative methane coupling. *Chem. Catal.* **2022**, *2*, 1775–1792. [CrossRef]
12. Chen, W.; Han, J.; Wei, Y.; Zheng, A. Frustrated lewis pair in zeolite cages for alkane activations. *Angew. Chem. Int. Ed.* **2022**, *61*, e202116269.
13. Chen, Y.; Wang, X.; Luo, X.; Lin, X.; Zhang, Y. Non-oxidative methane conversion using lead- and iron-modified albite catalysts in fixed-bed reactor. *Chin. J. Chem.* **2018**, *36*, 531–537. [CrossRef]
14. Xu, L.; Tian, J.; Wu, H.; Deng, W.; Yang, Y.; Sun, W.; Gao, Z.; Hu, Y. New insights into the oleate flotation response of feldspar particles of different sizes: Anisotropic adsorption model. *J. Colloid Interface Sci.* **2017**, *505*, 500–508. [CrossRef]
15. Scheidl, K.S.; Schaeffer, A.K.; Petrishcheva, E.; Habler, G.; Fischer, F.D.; Schreuer, J.; Abart, R. Chemically induced fracturing in alkali feldspar. *Phys. Chem. Miner.* **2013**, *41*, 1–16. [CrossRef]
16. Lu, A. Feldspar mineralogical effects of ultra-microchannel. *Bull. Miner. Petrol. Geochem.* **2007**, *26*, 194–195.
17. Wang, Z.; Liu, R. Characteristic research of micropores and microcracks in alkali feldspar. *Bull. Miner. Petrol. Geochem.* **2009**, *28*, 143–146.
18. Lu, A. Mineralogical effects of ultramicrochannel structures in natural selfpurification of inorganic minerals. *Acta Petrol. Miner.* **2005**, *24*, 503–510.
19. Shao, Y.; Zhang, J.; Li, Y.; Liu, Y.; Ke, Z. Frustrated lewis pair catalyzed C–H activation of heteroarenes: Astepwise carbene mechanism due to distance effect. *Org. Lett.* **2018**, *20*, 1102–1105. [CrossRef]
20. Zhang, S.; Zhang, M.; Qu, Y. Solid frustrated lewis pairs constructed on CeO₂ for small-molecule activation. *Acta Phys. Chim. Sin.* **2020**, *36*, 43–51.

21. Spies, P.; Schwendemann, S.; Lange, S.; Kehr, G.; Fröhlich, R.; Erker, G. Metal-free catalytic hydrogenation of enamines, imines, and conjugated phosphinoalkenylboranes. *Angew. Chem. Int. Ed.* **2008**, *47*, 7543–7546. [[CrossRef](#)] [[PubMed](#)]
22. Hamza, A.; Stirling, A.; Rokob, T.A.; Pápai, I. Mechanism of hydrogen activation by frustrated lewis pairs: A molecular orbital approach. *Int. J. Quantum. Chem.* **2009**, *109*, 2416–2425. [[CrossRef](#)]
23. Grimme, S.; Kruse, H.; Goerigk, L.; Erker, G. The mechanism of dihydrogen activation by frustrated lewis pairs revisited. *Angew. Chem. Int. Ed.* **2010**, *49*, 1402–1405. [[CrossRef](#)] [[PubMed](#)]
24. Nørskov, J.K.; Bligaard, T.; Hvolbaek, B.; Abild-Pedersen, F.; Chorkendorff, I.; Christensen, C.H. The nature of the active site in heterogeneous metal catalysis. *Chem. Soc. Rev.* **2008**, *37*, 2163–2171. [[CrossRef](#)]
25. Delley, B. An all-electron numerical method for solving the local density functional for polyatomic molecules. *Chem. Phys.* **1990**, *92*, 508–517. [[CrossRef](#)]
26. Perdew, J.P.; Burke, K.; Ernzerhof, M. Generalized gradient approximation made simple. *Phys. Rev. Lett.* **1996**, *77*, 3865–3868. [[CrossRef](#)]
27. Halgren, T.A.; Lipscomb, W.N. The synchronous-transit method for determining reaction path ways and locating molecular transition states. *Chem. Phys. Lett.* **1977**, *49*, 225–232. [[CrossRef](#)]
28. Jónsson, H.; Mills, G.; Jacobsen, K.W. Nudged Elastic Band Method for Finding Minimum Energy Paths of Transitions. In *Classical and Quantum Dynamics in Condensed Phase Simulations*; Berne, B.J., Ciccotti, G., Coler, D.F., Eds.; World Scientific: Singapore, 1998; p. 385.
29. Downs, R.T.; Hazen, R.M.; Finger, L.W. The high-pressure crystal chemistry of low albite and the origin of the pressure dependency of Al-Si ordering. *Am. Mineral.* **1994**, *79*, 1042–1052.
30. Delley, B. Hardness conserving semilocal pseudopotentials. *Phys. Rev. B* **2002**, *66*, 155125. [[CrossRef](#)]

Disclaimer/Publisher’s Note: The statements, opinions and data contained in all publications are solely those of the individual author(s) and contributor(s) and not of MDPI and/or the editor(s). MDPI and/or the editor(s) disclaim responsibility for any injury to people or property resulting from any ideas, methods, instructions or products referred to in the content.